

# Broadband and Fine-resolution Microwave Photonic Filtering with High-Speed Electronic Reconfigurability

Xinyi Zhu\*, Benjamin Crockett, Connor M. L. Rowe, and José Azaña

*Institut National de la Recherche Scientifique - Centre Énergie Matériaux Télécommunication (INRS-EMT),  
800 de la Gauchetière Ouest, Suite 6900, Montréal, H5A 1K6, QC, Canada*

\* Xinyi.zhu@inrs.ca

**Abstract:** We experimentally demonstrate electronically programmable, user-defined time-varying frequency filtering of continuous broadband signals, over a 22 GHz frequency tuning range and with  $>1$  GHz reconfiguration speed, using electro-optic modulation of a reversible time-mapped spectrogram.

## 1. Introduction

Time-varying linear filtering of highly non-stationary signals, in which the filter's frequency response can be reconfigured at a high speed, is increasingly needed for a wide range of applications in wireless communications, Radar/Lidar systems, biomedical signal processing etc. [1-3]. In order to precisely process the non-stationary signals found in the above-mentioned applications, such as to extract the desired signals from the background noise or interfering content, time-varying frequency filters with fully reconfigurable spectral transfer functions, enabling large tuning bandwidth ( $>10$ GHz) and high tuning speed (into the GHz range), are required. However, achieving all these specifications simultaneously remains very challenging. Linear filtering based on digital signal processing (DSP) of the detected waveforms e.g., using numerical Fourier post-processing, [4] can achieve time-varying frequency filtering with hyperfine frequency resolution; however, the real-time processing bandwidth of this conventional approach is inherently limited to below a few hundreds of MHz [5]. On the other hand, microwave photonic filters (MPFs) represent an interesting solution towards this aim as they offer important advantages in terms of broad operation frequency (or bandwidth), increased flexibility and reconfigurability, as compared with their conventional electrical filter counterparts [6]. However, present MPF filtering technologies are limited to reconfigurability speeds typically in the kHz range or slower. To overcome these limitations, photonic analog processing for continuous time-frequency (T-F) filtering of broadband signals, based on temporal imaging schemes, has been explored [7]. The technique reported in Ref. [7], based on a pulsed-Talbot spectrogram, enables joint time-frequency signal filtering at very high speeds but it is inherently limited to processing bandwidths up to a few GHz at best. Additionally, this specific method is constrained to the implementation of very simple spectral transfer functions, with only a few frequency analysis points (typically  $< 10$ ). No satisfactory time-varying filtering could be experimentally demonstrated using this approach. Thus, to our knowledge, no method has been reported that can perform a high-quality time-varying frequency filtering of an incoming broadband signal, with tens of GHz tuning range, and in a real-time manner, i.e., with a high tuning speed at least in the MHz range or above.

In this communication, we propose and experimentally demonstrate a novel, fully customizable time-frequency filtering technique enabling real-time dynamic transfer function control with unprecedented performance. The method involves a time-mapped spectrogram based on a temporal Talbot array illuminator (T-TAI), consisting of a discrete and bounded temporal phase modulation process followed by group-velocity dispersion, to access the time-frequency content of the high-speed waveforms in a continuous and gap-free fashion, and over a very broad bandwidth. The TAI

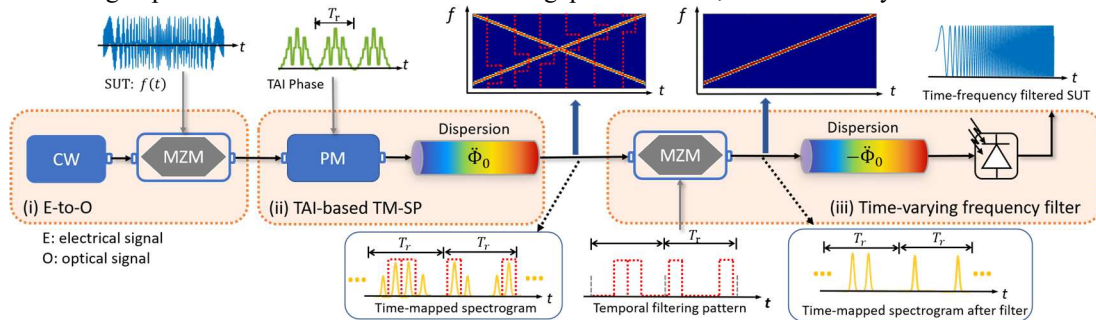


Fig. 1. Principle of the time-varying frequency filtering system. The scheme involves (i) converting the electrical signal to the optical domain (ii) TAI-based TM-SP and (iii) time-varying frequency filter. The dashed lines show the temporal filtering waveform designed to filter the target components (i.e., one of the chirp component) in the time-frequency domain.

spectrogram effectively implements the short-time Fourier transform (STFT) of the signal of interest with very high time and frequency resolutions, directly accessible along the time domain. As such, one can continuously process/filter the time-varying frequency components of the SUT using temporal manipulation mechanisms, e.g., by using an electro-optic modulator driven by an electronic arbitrary waveform generator (AWG) to program the desired spectral transfer function at will. Finally, the filtered signal can be simply recovered through a dispersion compensation medium followed by a photodetector. To showcase the unique performance advantages offered by this method, we report user-defined time-varying frequency filtering with a tuning speed of  $\sim 1.3$  GHz, over a microwave signal bandwidth up to  $\sim 23$  GHz (i.e., 46-GHz full optical bandwidth), and with about 35 frequency processing points.

## 2. Operation Principle

As illustrated in Fig.1, the proposed time-varying frequency filtering system involves a cascade of the following elements: (i) electro-optic conversion of the SUT, (ii) Talbot array illuminator-based time mapped spectrogram (TM-SP) unit, and (iii) a time-varying frequency (T-F) filter and signal regeneration unit. The microwave signal under test (SUT) is first modulated on a continuous wave (CW) optical carrier centered at 1553.5 nm using a Mach-Zehnder modulator (MZM, 40 GHz bandwidth). The optical SUT then enters the TAI spectrogram unit, composed of an electro-optic phase modulator (PM, 40 GHz bandwidth and 3.2 Volts  $V_\pi$ ) driven by an AWG (92 GSa/s) providing the needed multi-level phase pattern, where the  $n^{\text{th}}$  phase step follows  $\phi_n = -\pi n^2(q-1)/q$ , for  $n=1 \dots q$  [8]. Specifically, the modulation phase profile consists of  $q$  phase levels and the length of each level is  $t_s$ , forming a periodic pattern of period length  $T_r = qt_s$ . The analysis bandwidth is determined by the inverse of the duration of a single phase step,  $\Delta\omega_s \sim 2\pi/t_s$ , while the temporal resolution  $\delta t_{res}$  of the implemented STFT analysis is approximately given by the period of the phase pattern  $T_r$ , which is inversely related to the frequency resolution and tuning speed. This phase-modulated signal then propagates through a dispersive element providing a second-order dispersion satisfying  $2\pi|\ddot{\phi}| = qt_s$ . The output temporal signal of the dispersive element corresponds to the time-mapped spectrogram, which maps the varying frequency spectrum of the incoming SUT along the time domain. In particular, the spectra of consecutive truncated sections of the SUT are mapped along consecutive time windows with a period of  $T_r$ , and according to the frequency-to-time mapping law  $\Delta\omega_t \rightarrow \Delta t/|\ddot{\phi}|$ , where  $\Delta\omega_t$  and  $\Delta t$  are relative to the center of each analysis window. Subsequently, a user-defined temporal pattern is used to modulate the time-mapped spectrogram through a second MZM (40 GHz bandwidth and 37 dB extinction ratio). As the time-changing spectrum of the SUT is continuously mapped along the time domain, one can extract or eliminate the target frequency components along each time slot by suitably designing the temporal filtering function, according to the above time-to-frequency mapping

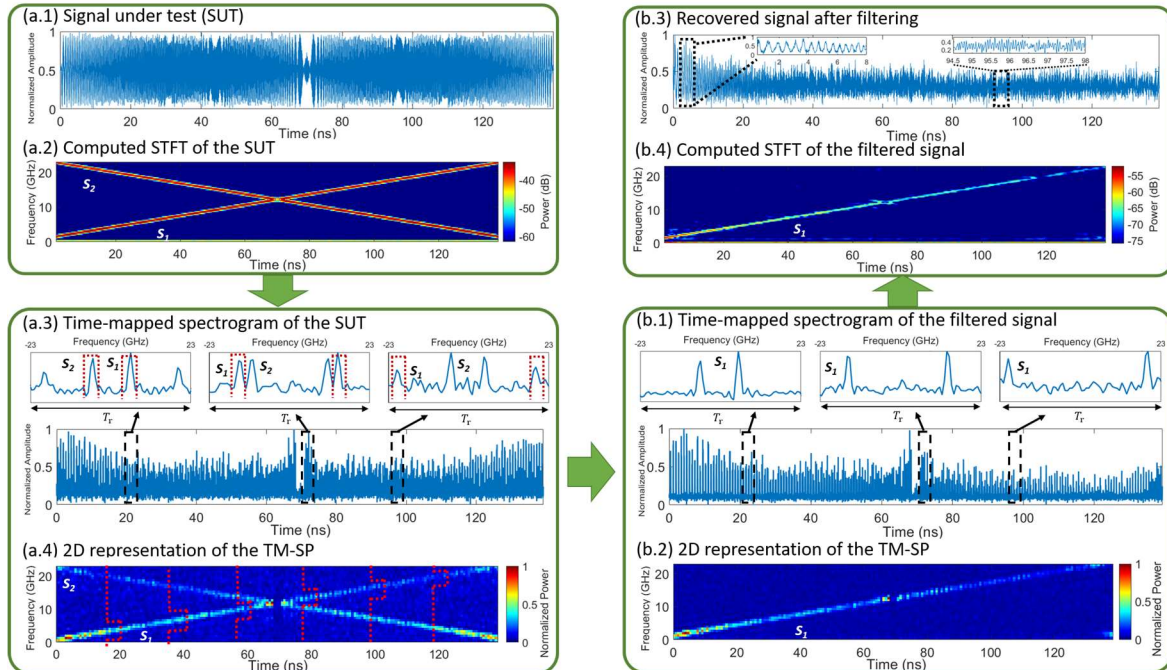


Fig. 2. Experimental results. (a.1) Numerical temporal waveform of the SUT. (a.2) Numerical STFT spectrogram of the SUT. (a.3) The temporal waveform at the output of the TAI-based TM-SP, along with the temporal filtering waveform (dashed). (a.4) 2D representation of the TM-SP along with the gating waveform. (b.1) The TM-SP after T-F filtering. (b.2) 2D representation of the filtered TM-SP. (b.3) The recovered signal after the second dispersive element. (b.4) Numerical STFT spectrogram of the recovered signal.

factor, thus implementing the desired T-F filtering process. As a result, the tuning speed of the T-F filter is determined by the analysis period  $T_r$  of the TM-SP. The operation bandwidth and frequency resolution of the time-frequency processor corresponds to those of the TM-SP. The resulting filtered signal is then recovered by propagation through a second dispersive line with the exact opposite dispersion of the first one, i.e.,  $-\phi$ . Finally, the recovered signal is converted back into the microwave domain using a high-speed photodiode (PD).

### 3. Experimental Results

To demonstrate the time-frequency dynamic filtering capabilities of the proposed scheme, we target filtering out a chirp component from a double-chirped signal, shown in Fig. 2. Specifically, we design a  $\sim 140$ -ns long microwave SUT, which is composed of two superimposed linearly-chirped sinusoidal waveforms, one varying from 1.34 GHz to 23 GHz and vice versa for the other, labeled  $S_1$  and  $S_2$ , respectively. This signal exhibits then a total optical bandwidth of  $\sim 46$  GHz. The digitally generated waveform that was sent to the AWG for generation of the SUT and the measured modulated signal are shown in Fig. 2(a.1), whereas the intensity of its numerically computed short-time Fourier transform (STFT) is shown in Fig. 2(a.2). To analyze this signal using the TAI spectrogram, we set the analysis bandwidth to  $46 \text{ GHz} \sim 1/t_s$  and employ a linearly chirped fiber Bragg grating (LCFBG) to provide a second-order dispersion  $\phi \sim 2,600 \text{ ps}^2/\text{rad}$ . This sets the analysis period to  $T_r \approx 0.76 \text{ ns}$ , corresponding to a frequency resolution of 1.3 GHz, allowing for a total of 34 analysis points per spectrum. Fig. 2(a.3) shows the measured output temporal waveform of the TAI spectrogram, with zoomed-in regions over different analysis periods, each with a duration of  $T_r$ . As predicted, the temporal mapping clearly shows the two different frequency components of the SUT (i.e.,  $S_1$  and  $S_2$ ) along each analysis window. The 2D representation in Fig. 2(a.4) was obtained from the output temporal trace by vertically plotting adjacent analysis windows and setting the frequency axis according to the frequency-to-time mapping law defined above. This representation clearly depicts the evolving frequency content of the two chirps. The TM-SP is then processed by the time-varying filter as follows. The temporal filtering pattern (i.e., rectangular passbands, dashed red trace) is designed to select only one chirped waveform (i.e.,  $S_1$ ) from the two crossed chirps. This is done by dynamically varying the filter with a tuning speed of  $\sim 1.3 \text{ GHz}$  and using an  $\sim 25$ -ps pulse width, corresponding to a filter passband equal to the frequency resolution of the TM-SP (i.e.,  $\sim 1.3 \text{ GHz}$ ). Thus, the transfer-function profiles for the filter are programmed to select the desired linear chirped frequency components in every analysis time window  $T_r$ , implementing the target time-variant filtering function. Fig. 2(b.1) shows the measured T-F filtered waveform at the output of the second MZM. Notice that as designed, only the pulses representing the frequency components of  $S_1$  are maintained. The corresponding 2D representation of this TM-SP is shown in Fig. 2 (b.2), again showing a clear decimation of the unwanted chirp. Finally, the T-F filtered temporal waveform is recovered after the second LCFBG, providing the exact opposite dispersion to the first LCFBG used for the TAI spectrogram. The recovered microwave signal is measured using a 50-GHz PD connected to a 28-GHz real-time oscilloscope, shown in Fig. 2(b.3). The corresponding numerical spectrogram is also shown in Fig. 2 (b.4). Compared with the input, the output STFT spectrogram clearly confirms that the unwanted signal with decreasing frequency-chirp has been successfully decimated using the proposed T-F filtering system.

### 4. Conclusions

We have proposed and experimentally demonstrated a fully reconfigurable scheme for time-varying frequency filtering of broadband microwave signals, which operates in real-time and allows for unprecedented performance and processing capabilities. We have demonstrated the broad frequency range tunability and high (GHz range) tuning speed of the proposed approach by filtering a  $\sim 140$ -ns single linearly chirped signal (1.34 GHz  $\sim$  23 GHz) from a dual chirped input signal. We envision numerous applications for this new class of highly reconfigurable microwave photonic filters, towards realization of the software-defined information and communication technology paradigm.

### 5. References

- [1] J. Capmany, B. Ortega, and D. Pastor, "A tutorial on microwave photonic filters," *J. Lightwave. Technol.* **24**, 201–229 (2006).
- [2] Y. I. Al-Yasir, et al., "Recent progress in the design of 4G/5G reconfigurable filters," *Electronics* **8**, 114 (2019).
- [3] B. Boashash, "Time-Frequency Signal Analysis and Processing: A Comprehensive Reference," (Academic press, 2015).
- [4] Y. Xie, et al., "Programmable optical processor chips: toward photonic RF filters with DSP-level flexibility and MHz-band selectivity," *Nanophotonics* **7**, 421–454 (2018).
- [5] X. Xie, et al., "STFT based on bandwidth-scaled microwave photonics," *J. Lightwave. Technol.* **39**, 1680–1687 (2020).
- [6] M. P. Fok, and J. Ge, "Tunable multiband microwave photonic filters," *Photonics* **4**, 45 (2017).
- [7] S. R. Konatham, and J. Azana, "On-the-fly continuous time varying frequency filtering of broadband microwave signals," 45th European Conference on Optical Communication (ECOC 2019).
- [8] B. Crockett, et al., "Optical signal denoising through temporal passive amplification," *Optica* **9**, 130–138, (2022).